Rapid characterization of a Delta-Omicron SARS-CoV-2 recombinant detected in Europe

Etienne SIMON-LORIERE (etienne.simon-loriere@pasteur.fr)
Institut Pasteur https://orcid.org/0000-0001-8420-7743

Xavier Montagutelli
Institut Pasteur https://orcid.org/0000-0002-9372-5398

Frederic Lemoine
Institut Pasteur https://orcid.org/0000-0001-9576-4449

Flora Donati
Institut Pasteur https://orcid.org/0000-0003-2862-9751

Franck Touret
UVE Aix Marseille Univ, IRD 190, INSERM 1207, IHU Méditerranée Infection https://orcid.org/0000-0002-4734-2249

Jerome Bourret
Institut Pasteur

Matthieu Prot
Institut Pasteur

Sandie Munier
Institut Pasteur

Mikael Attia
Institut Pasteur

Laurine Conquet
Institut Pasteur

Scott Nguyen
District of Columbia https://orcid.org/0000-0001-6498-2232

faustine amara
institut pasteur

Anna Maisa
Santé publique France

Lucie Fournier
Santé publique France

Angela Brisbarre
Institut Pasteur

oceane dehan
institut pasteur

Laurine Levillayer
Institut Pasteur
Vithiagaran Gunalan
Statens Serum Institut
The Danish COVID-19 Genome Consortium (DCGC)
Statens Serum Institut
Jannik Fonager
Department of Virus & Microbiological Special Diagnostics, Statens Serum Institut
https://orcid.org/0000-0003-1688-1482
Morten Rasmussen
Department of Virus & Microbiological Special Diagnostics, Statens Serum Institut
Stephan Kemeny
Inovie GEN-BIO
Abdelali Zrhidri
Inovie GEN-BIO
Thomas Duret
Inovie GEN-BIO
Sylvie Behillil
Institut Pasteur
Vincent Enouf
Pasteur Institute
Christophe Rodriguez
Hôpital Henri Mondor
Slim Fourati
Hôpital Henri Mondor
Jean-Michel Pawlotsky
Hôpital Henri Mondor
Nicolas Capron
BioPath
Hugues Leroy
BioPath
Elodie Alessandri-Gradt
CHU Rouen https://orcid.org/0000-0002-8906-3416
Florian Juszczak
National Platform bis UMONS
Laetitia Gheysen
National Platform bis UMONS
Véronique Brodard
Hôpital Robert Debré

Hélène Moret
Hôpital Robert Debré
Martine Bos
inBiome B.V.
Matthijs Welkers
Public Health Service Amsterdam
Claus Scholz
Laboratory Dr. Wisplinghoff https://orcid.org/0000-0002-6406-7859
Sofia Paraskevopoulou
Robert Koch Institute
Laurence Josset
CHU Lyon
Claire Cervi
Laboratoires Corcy et associés
Brigitte Couzon
Centre Hospitalier de Versailles
Stéphanie Marque-Juillet
Centre Hospitalier de Versailles
Deborah Delaune
Institut Pasteur https://orcid.org/0000-0003-4970-9566
Slim El Khiari
Institut Pasteur
Julien Fumey
Institut Pasteur
Marie-Charlotte Hallouin-Bernard
Institut Pasteur
Félix Rey
Institut Pasteur https://orcid.org/0000-0002-9953-7988
Yazdan Yazdanpanah
ANRS-MIE
Bruno Coignard
Santé publique France
Xavier de Lamballerie
UMR Émergence des Pathologies Virales (EPV: Aix-Marseille Université – IRD 190-INSERM 1207 – EHESP – IHU Méditerranée Infection), Marseille, France https://orcid.org/0000-0001-7895-2720
Sylvie van der Werf
Institut Pasteur https://orcid.org/0000-0002-1148-4456
Axelle Paquin
Centre Hospitalier de Laval

Biological Sciences - Article

Keywords:

Posted Date: April 4th, 2022

DOI: https://doi.org/10.21203/rs.3.rs-1502293/v1

Abstract

Recombination is a crucial process in the evolution of many organisms. Although the evolutionary reasons behind its occurrence in RNA viruses are debated, this phenomenon has been associated with major epidemiological events such as virus host range expansion, antigenic shift or variation in virulence 1,2, and this process occurs frequently in positive strand RNA viruses such as coronaviruses. The SARS-CoV-2 pandemic has been associated with the repeated emergence of variants of concern presenting increased transmissibility, severity or immune escape 3. The recent extensive circulation of Delta worldwide and its subsequent replacement by viruses of the Omicron lineage 4 (BA.1 then BA.2), have created conditions for genetic exchanges between viruses with both genetic diversity and phenotypic specificities 5-7. Here we report the identification and in vitro and in vivo characterization of a Delta-Omicron recombinant in Europe. This recombinant exhibits immune escape properties similar to Omicron, while its behavior in mice expressing the human ACE2 receptor is more similar to Delta. This recombinant provides a unique and natural opportunity to better understand the genotype to phenotype links in SARS-CoV-2.

Main

The recombination process can occur when two genetically distinct viruses co-infect a cell, and corresponds to the generation of a chimeric molecule classically as a result of template switching during replication, although other mechanisms exist. The divergence between the parental sequences and the length of the genomic regions involved strongly affect the possibility to detect such events. In addition, recombination may bring together genetic variations that will not necessarily result in a functional and fit virus, as short- or long-distance epistatic interactions in the genome and proteins might be disrupted. The mechanistic process is thus likely much more frequent than the – epidemiologically relevant – fraction that can be captured by genomic surveillance.

There is potent evidence that recombination is pervasive in the evolutionary history of many viral families, including coronaviruses and the sarbecovirus subgenus to which SARS-CoV-2 belongs [8,9]. There are similarly increasing reports on the frequent occurrence of recombination throughout the COVID-19 pandemic [10-13].

Identification of a recombinant and putative parent lineages in Europe

In early 2022, multiple laboratories contributing to routine SARS-CoV-2 genomic surveillance in France (the EMERGEN consortium) and in Europe, publicly shared sequences initially classified as Delta AY.4 and 21J by Pangolin [14] and Nextclade [15] respectively. Further examination of these genomes revealed a large number of signature mutations characteristic of the BA.1 lineage in only a portion of the genome, highly suggestive of a recombinant [16]. Analysis of the raw sequencing data of primary samples and of an isolate revealed the absence of co-infection or contamination and the correct assembly of the genome

(see methods). The lineage was designated as clade GKA by GISAID, then received the Pango lineage designation XD and was classified as a variant under monitoring by ECDC on March 17, 2022 [17].

The mosaic structure of the genome is described in Fig. 1 and Extended Data Fig. 1. We identified two breakpoints, one at the beginning of the spike (in a window spanning nt 22035 to 22194) and one within ORF 3a (nt 25469 to 25583). At the time of writing, the earliest sequence of this recombinant was sampled on January 3rd, 2022 in Northern France during routine surveillance (random selection for sequencing of a fraction of weekly cases, "Flash investigation"). As of March 18th, 2022, the XD lineage has been detected in multiple regions of France, as well as in Denmark, the Netherlands, Belgium and Germany, through random sampling and cluster investigations. The majority of cases investigated reported no travel history, except for one case travelling from Italy, suggesting widespread but infrequent circulation. In support of this, we observed signal of diversification within the lineage, with geographic clustering within both France and Europe (Fig. 1b,c).

Data from ongoing epidemiological investigations were available from 32 confirmed XD cases and six suspected cases who tested positive for SARS-CoV-2 between January 3rd and March 9th, 2022 in France (Extended Data Fig. 2a). As comparison, we used epidemiological data recently obtained from investigations of Omicron (BA.1) cases with the same methodology in France [18]. The median age was 32.5 years (IQR 19.75-44.75), which was similar to Omicron cases (35 years), however, significantly more XD cases were below 20 years of age (25.7%) compared to Omicron cases (11.3%, p = 0.026, Extended Data Fig. 2b). Only two XD cases reported a previous SARS-CoV-2 infection (5.6%, Table 1), fewer than for Omicron (14%). No XD case was over 70 years old, and no risk factor was reported. Only 6% of recombinant cases were unvaccinated (vs 27% for Omicron cases), and 30% had received three doses (vs 8%), but the overall vaccination coverage of the population was different between the XD and Omicron study periods. All XD cases reported here from France were symptomatic and most reported symptoms were headache (61.1%), asthenia/fatigue (58.3%), cough (44.4%), fever (38.9%) and myalgia (33.3%, Extended Data Fig. 2b). The main differences compared to Omicron cases were the higher rates of ageusia (odds ratio OR 2.71 [1.064-6.514], p=0.024) and anosmia (OR 1.98 [0.66-5.251], p = 0.18). Two XD cases were hospitalized, one for unrelated causes, but for less than 24h and without intensive care admission.

Search for the putative parental sequences

Splitting conservatively the genome based on the largest breakpoint windows, we performed similarity searches on the GISAID [19] EpiCoV database to identify (closely related) genomes that may represent the lineages that gave rise to this recombinant virus. While the shorter region inherited from BA.1 returned a large set of genomes from all over the world, likely due to the shorter genomic portion involved and the relatively low diversity of the recently emerged BA.1, the Delta-like part of the genome led to a small subset of sequences (n=69) within the large AY.4 sublineage. The closest relatives were predominantly

sampled in Europe (France, Germany and Sweden, Extended Data Fig. 3). Together with the closest detected AY.4 genomes, the recombinant XD lineage (with the Omicron part of the genome masked) forms a monophyletic cluster (branch support: 0.98).

Growing reports of potential SARS-CoV-2 recombinant sequences describe mosaic genomes with breakpoints recurrently noted in specific regions of the genome such as the beginning of the spike. Similar observations can be made in the evolutionary history of the family *Coronaviridae*, and hotspots of recombination have been described for other viruses such as HIV-1 or poliovirus [20,21]. However, the relative rarity of the candidate AY.4 parental sublineage suggests that all currently reported XD viruses likely derive from a unique ancestor.

We isolated a representative virus of each of the parental lineages, as well as a recombinant XD virus, allowing to further demonstrate the recombinant genotype. The selected AY.4 virus, sampled in Ile-de-France on December 27, 2021, presented 100% identity with the Delta-like region, and the BA.1 virus was similarly 100% identical to the Omicron-like region of the XD virus. Importantly, this allowed us to rapidly characterize the recombinant virus in comparison to representatives of the parental lineages using primary isolates, and gain insights into determinants of the phenotypic differences between the variants of concern (VOCs) Delta and Omicron BA.1.

Sensitivity of XD to sera from vaccinees

Many of the unique properties of Omicron have been tied to the extensive changes that accumulated in the spike in comparison to the ancestral SARS-CoV-2 sequence. Omicron has been proposed to be considered a distinct strain of SARS-CoV-2, and the use of a serotype classification has been discussed [22]. As the XD spike carries a larger fraction of the signature changes of BA.1, including the entirety of the receptor binding domain (RBD) (Extended Data Fig. 4), we hypothesized that this recombinant might present similar immune escape properties [23,24]. To assess this, we generated pseudoviruses expressing the XD spike, and compared the neutralizing activity of sera from vaccinated individuals, using the ancestral, Delta (AY.4), and Omicron (BA.1) spikes as reference. Our panel included sera sampled at 1 or 6 months after the last immunization, from individuals infected and vaccinated with the Pfizer vaccine or vaccinated with either 2 doses of the Pfizer vaccine, the AstraZeneca vaccine or a combination of both, or including a booster of the Moderna vaccine (Table 2).

As described previously, we observed only a small reduction in the neutralizing titers against Delta compared to the ancestral virus. In contrast, both the XD recombinant and BA.1 were barely neutralized by sera sampled 1 or 6 months after 2 doses. The titers were all much higher 1 month after a third immunization, although they displayed an 8-fold to 10-fold reduction in neutralization efficacy against both BA.1 and XD compared to the original virus. Likewise, in individuals infected and vaccinated with one dose, neutralization titers towards BA.1 and XD were reduced 3.4- and 3.7-fold (but not significant differences), respectively. These results were obtained with a pseudovirus assay, which has been shown

to be strongly correlated with infectious virus experiments, but it cannot be excluded that differences in susceptibility or escape to neutralization do exist for this chimeric virus.

Taken together, these results indicate that XD displays immune escape properties similar to those of BA.1, and further reinforce the major role of the spike RBD epitopes in the vaccine induced neutralizing response in our serum panel.

Neutralization of Omicron by monoclonal antibodies

We next assessed the sensitivity of the XD recombinant to a panel of therapeutic COVID-19 human monoclonal antibodies using infectious viruses. We selected monoclonal antibodies that are currently in clinical use and have been associated with varying reduction of activity against Omicron BA.1 [24,25]. We included putative parental viruses (AY.4 and BA.1) and a B.1 isolate (carrying the spike D614G substitution) for comparison.

Consistently with the binding targets of our antibodies, which correspond to sequences that are identical between the parental BA.1 and recombinant virus, we observed highly similar reductions in neutralizing activity for these viruses, and distinct from the AY.4 parental virus. As against BA.1, Tixagevimab lost all detectable neutralizing potential against the XD virus, and Cilgavimab conserved a neutralizing activity with a shift in EC_{50} from 29.7 ng/mL against B.1 to 402.8 ng/mL (fold change reduction of 13.5 for XD vs 16.9 for BA.1) (Table 3). The combination of these antibodies, proposed as the Evusheld cocktail, accordingly, presented strongly reduced activity (fold change reduction of 37.9 for XD vs 36.7 for BA.1), while Delta AY.4 was neutralized as efficiently as the B.1 virus. As reported previously, Sotrovimab showed a small reduction (2.6-fold) in activity against BA.1 [24,25], which was somewhat more pronounced against the XD virus (5.1-fold reduction).

These results indicate that the XD recombinant, which possesses the RBD and S2 of Omicron BA.1, shares the escape properties of the latter, and does not complexify the landscape of vaccines and therapeutic efficacy.

XD recombinant is not attenuated in a mouse model of infection

Although it is challenging to infer the intrinsic severity of novel SARS-CoV-2 variants as they circulate in populations with significant proportion of immunity with varying levels, Omicron BA.1 has been associated with lower risks of severe disease compared to Delta [26,27]. Consistently, BA.1 has been shown to cause attenuated disease in rodent models, including in the highly susceptible model of human ACE2 transgenic (K18-hACE2) mice [28,29].

We infected K18-hACE2 mice with $2x10^4$ PFU of either the recombinant or each parental lineage virus. We first compared the viral load in the lungs and nasal turbinates at 3 days post-infection (dpi). The levels of viral RNA in the lungs of mice infected with BA.1 or XD viruses were comparable, and 3.7-fold lower than those of AY.4-infected animals (Fig. 3a). In contrast, the viral load in nasal turbinates of the XD-infected

mice was 8.5-fold higher than that in BA.1-infected animals, and only slightly lower than that of AY.4 infected mice. Similar differences were noted when measuring infectious titers (Fig. 3b).

We also monitored mice for body weight loss and disease over 11 days (Fig. 3c,d, Extended Data Fig. 5). Like the main Delta lineage, the parental AY.4 isolate resulted in disease with weight loss that accelerated at 3 dpi, and 6/7 mice reached humane endpoints between dpi 7 and 9. As described, BA.1 infection was not associated with weight loss nor lethality. With the XD virus, we did not observe weight loss during the first 5 dpi, but all mice deteriorated rapidly between day 5 and 8 and died or had to be euthanized by day 9. Clinical scores followed the same progression and delayed onset in XD- compared with AY.4-infected mice.

Together, these results indicate that the Delta-Omicron XD recombinant is associated with clinical features distinct from those of Omicron BA.1 in K18-hACE2 mice. It further suggests that the attenuated phenotype of BA.1 in this model cannot be only linked to the variations in the spike such as in the RBD or near the furin cleavage site. Further experiments will be needed to determine the basis of the XD recombinant intermediate phenotype in mice and to determine how this relates to XD infection in humans.

In vivo replication

To further investigate potential differences in the replicative fitness of viruses of the XD lineage, we measured its growth in comparison to Omicron BA.1, which was the dominant lineage in France and most of Europe at the time of initial detection of the recombinant. As competition experiments may expose differences in replication efficacy that are not detected in individual growth kinetic assays, we inoculated groups of K18-hACE2 mice with a mixture of BA.1 and XD viruses at 1:1, 1:9 or 9:1 ratio and used metagenomic sequencing to estimate the ratio of the viral genomes at 3dpi in both the lungs and the nasal turbinates (Fig.3e). While BA.1 consistently outcompeted the XD recombinant in the lungs, the reverse was observed in the nasal turbinates, both results being in accordance with what was observed with each virus separately.

Taken together, these results indicate that XD and BA.1 each present a replicative advantage in different environments. The apparent superior fitness of XD compared to Omicron BA.1 in the upper airways of K18-hACE2 mice suggests that this trait is not tied to the spike RBD nor its furin cleavage efficacy. Variations present in the first part of the spike N-terminal domain (from AY.4 in XD) might contribute to these differences if related to the entry process itself. However, other specificities present in the genome and in both structural and non-structural proteins might be involved in the XD phenotype (Extended Data Fig. 6).

Potential limitations of our work include the low number of confirmed cases of XD virus infections, in a context of overall high incidence and evolving testing strategies in Europe, potentially limiting the ability to detect variants in asymptomatic cases. The pathogenicity and transmission potential in humans thus remain unclear. The K18-hACE2 mouse model used here is highly susceptible to SARS-CoV-2 infection,

and importantly does not include any pre-existing immunity to the virus, which has been shown to considerably reduce the risk of severe COVID-19. In addition, considering that the XD lineage has been circulating at least since the beginning of January 2022, and although this lineage has been captured by random genomic surveillance in multiple European countries, the limited detection might reflect the inability of this lineage to outcompete Omicron BA.1 and BA.2 in human populations. Further work is needed to dissect the epidemiological and virological characteristics of the XD recombinant.

The continued diversification observed during the COVID-19 pandemic, with the extreme case of the emergence of VOCs and their intense circulation, is likely to provide further opportunities for recombination, and continued worldwide monitoring and rapid risk assessment will be crucial to our long-term response to SARS-CoV-2 circulation and understanding of its biology.

Methods

Virus sequencing

The consensus genome sequences of SARS-CoV-2 lineage XD / clade GKA described here have all been deposited on the GISAID EpiCoV database (EPI_SET_20220325yn), and have been generated by different PCR amplification strategies and on either Illumina or Oxford Nanopore technologies platforms, as described in their sequences entries. We also deposited raw reads data (GISAID ID: EPI_ISL_9879437 and EPI_ISL_9879436, with human host reads removed) for two primary samples generated by the National Reference Center for Viruses of respiratory infection hosted at Institut Pasteur and part of the Emergen consortium. These data were generated using a highly multiplexed short PCR amplicon approach (panel ARTIC V4.1) [30], followed by library preparation with the Nextera XT kit. Viral stocks were verified by untargeted metagenomic sequencing. RNA was extracted from culture supernatant, converted into double stranded cDNA and libraries were prepared using the Nextera XT kit. Both genomic surveillance and virus stocks libraries were sequenced on an Illumina NextSeq500 (2x150 cycles) at the Mutualized Platform for Microbiology.

For the competition assays readout, we used an untargeted metagenomic sequencing approach with ribosomal RNA (rRNA) depletion, which has been shown to capture the diversity of RNA species present within a sample [31]. RNA was extracted with the QIAamp Viral RNA extraction kit (Qiagen), with the poly-A RNA carrier provided. Prior to library construction, carrier RNA and host rRNA were depleted using oligo (dT) and custom probes respectively. The RNA resulting from selective depletion was used for random-primed cDNA synthesis using the SuperScript IV RT (Invitrogen). Second-strand cDNA was generated using Escherichia coli DNA ligase, RNAse H and DNA polymerase (New England Biolabs) and purified using Agencourt AMPure XP beads (Beckman Coulter). Libraries were then prepared using the Nextera XT kit and sequenced on an Illumina NextSeq500 platform (2x75 cycles).

Investigation of sequencing reads data

To rule out the possibility that the consensus sequences of XD lineage viruses correspond to coinfection or contamination, we examined the raw read data generated by multiple platforms and approaches, to estimate the frequency of intrahost single nucleotide variants (iSNVs) at all positions along the genome, with a focus on positions that differs between the Delta and Omicron variants. We used iVAR [32] and thus SAMtools [33] to compute the nucleotides frequencies. For comparison, we computed the same statistics for samples that were rejected as possible contamination or coinfection by our sequencing curation pipeline. The raw reads of samples hCoV-19/France/HDF-IPP04947/2022, hCoV-19/France/HDF-IPP08027/2022 (amplicons), as well as direct metagenomic sequencing of the XD isolate viral stock (hCoV-19/France/HDF-IPP08027i/2022) have been deposited on GISAID (EPI_SET_20220320tx). Representative examples are shown in Extended Data Fig. 7.

Epidemiological investigations

Confirmed cases were defined as patients with a positive SARS-CoV-2 test and a sequencing result demonstrating infection by recombinant XD. Suspected cases were defined as patients with a positive SARS-CoV-2 test and an epidemiological link with a confirmed case. Cases were interviewed by the Regional offices of Santé publique France (SpF, the French national Public Health Agency) using a standard questionnaire. Collected data included demographic information (sex, age, place of residence), travel history, contact persons, vaccination status, symptoms and outcome. The earliest XD case was a family contact of a case with recent travel to Niger, and one case reported recent travel to Italy. A similar investigation was performed during the emergence of Omicron (mostly BA.1) in France [18] and was used for comparison.

Identification of putative parental sequences

To identify putative parental genome sequences, we retrieved all SARS-CoV-2 sequences available on the GISAID EpiCoV database as of March 9th, 2022. We did not restrict our search to a window of time corresponding to the earliest detection of BA.1 to the days prior to the earliest available sequence of lineage XD, to be able to capture all possible related genomes of the parental lineages. We reduced this dataset to sequences longer than 28000 nt and including less than 5% of Ns, on which we performed a similarity search using gofasta (https://github.com/cov-ert/gofasta). As a query, we used XD genomes after masking either the region corresponding to the AY.4-like or to the BA.1-like part of the genome.

Specifically, we set the boundary coordinates to the ends of sequential tracts of mutations specific to the putative parental sequences. This is a conservative approach to assigning parental lineages and consequently no parental lineage is assigned to those genome regions that do not contain unambiguous lineage-defining mutations or deletions.

We conservatively masked the entirety of the breakpoint windows in each case, and the genome extremities (keeping nt 101- 22034 and 25584-29802 for the AY.4 search, and 22193-25469 for the BA.1 search). All numberings are based on the Wuhan-Hu-1 reference genome (GenBank ID: NC_045512). The AY.4 search resulted in 69 sequences post quality filtering. For BA.1, we restricted our selection to

sequences 100% identical to our recombinant query, resulting in 39557 sequences. We also selected all sequences belonging to AY.4 lineage or one of its sub-lineages (995977 sequences), after annotating the sequences with Pangolin (v3.1.20, pangolearn 2022-02-28, scorpio v0.3.16, constellation, v0.1.3, pangodesign v1.2.32) with Usher placement.

We compiled statistics for each position of the sequences sets. We also inferred maximum likelihood phylogenies for each putative parental sequences dataset (randomly subsampled for the related BA.1 genomes) (Extended Data Fig. 3).

Single nucleotide differences between the XD recombinant sequences and closely related putative parental sequences were visualized using snipit (https://github.com/aineniamh/snipit), Extended Data Fig. 3. Analysis of the variations within the putative parental AY.4 sublineage suggests that the breakpoint window at the beginning of the spike could be further reduced to nt 22035 to 22096, as the closest AY.4 sequences all carry an A at position 22097 (C in the recombinant sequences).

Phylogenetic analysis

To analyze the recombinant genomes, we generated a contextual dataset representative of the global circulation of SARS-CoV-2 since its emergence using the subsampling strategy implemented in Nextstrain (v.3.0.5) [34]. We added high quality XD genomes (n = 16) reported here, as well as subsets of the AY.4 (n = 29) and BA.1 (n= 30) genomes identified by similarity search (EPISET EPI_SET_20220324xe).

As in the similarity search, we also used versions of the recombinant genomes where either one of the regions with distinct ancestry was masked. To characterize the genetic diversity of lineage XD, the complete genome was used, and the reference genome added to root the phylogeny.

Maximum-likelihood phylogenies were inferred using IQ-TREE v2.0.6 and branch support was calculated using ultrafast bootstrap approximation with 1000 replicates [35,36]. Prior to the tree reconstruction, the ModelFinder application [37], as implemented in IQ-TREE, was used to select the best-fitting nucleotide substitution model. The resulting phylogenies were visualized using Auspice v.2.29.1 and Figtree v.1.4.4 (http://tree.bio.ed.ac.uk/software/figtree/).

We separately downsampled this dataset to perform recombination analyses using methods implemented in RDP5 [38], including 3SEQ [39], confirming the clear signal for the two recombination breakpoints.

Cell lines

VeroE6 cells (African green monkey kidney cells from ATCC (CCL-81)), were maintained in Dulbecco's Modified Eagle's Medium (DMEM, Life Technologies) supplemented with 5% fetal bovine serum (FBS) and penicillin/streptomycin. VeroE6/TMPRSS2 cells (ID 100978) were obtained from CFAR and were maintained in minimal essential medium (Life Technologies) with 7.5% heat-inactivated fetal calf serum, 1% penicillin/streptomycin and G-418 (Life Technologies). Human embryonic kidney HEK-293T (ATCC

CRL-3216) and HEK-293T cells stably expressing human ACE2 (293T-ACE2) were maintained in DMEM supplemented with 10% FBS and penicillin/streptomycin.

Viral Isolates

We isolated the XD virus and the putative parental AY.4 virus from nasopharyngeal swabs received in the context of our random genomic surveillance. The sequences of the swabs and the outgrown viruses (XD: EPI_ISL_10819657 and AY.4: EPI_ISL_11373018) were identical. All SARS-CoV-2 isolates were supplied by the National Reference Centre for Respiratory Viruses hosted at Institut Pasteur (Paris, France). The human sample from which XD strain hCoV-19/France/HDF-IPP08027i/2022 was isolated has been provided by Dr. Jean-Marc Corcy Laboratoire Corcy et Associés, Soissons, France (hCoV-19/France/HDF-IPP08027/2022 GISAID ID: EPI_ISL_9879437). The human sample from which the AY.4 virus hCoV-19/France/IDF-IPP52092i/2021 was isolated has been provided by Dr. Stéphanie Marque-Juillet, CH de Versailles, France (hCoV-19/France/IDF-IPP52092/2021 GISAID ID: EPI_ISL_8546521). The human sample from which the BA.1 virus hCoV-19/France/PDL-IPP46934/2021 was isolated has been provided by Dr. Axelle Paquin, CH de Laval, France (GISAID ID: EPI_ISL_8588473).

Virus isolation was performed on VeroE6 cells in the presence of 1 µg/mL TPCK trypsin as previously described [40], followed by 2 passages on VeroE6 cells at a MOI of 10-4 to obtain a viral stock. We performed metagenomic sequencing on the sample to check the presence of potential contaminants and verify if the virus had acquired genomic changes during isolation, and each isolate sequence was identical to the primary isolate sequence. All work with infectious virus was performed in biosafety level 3 containment laboratories.

SARS-CoV-2 isolate B.1 (BavPat1 EPI_ISL_406862) was obtained from Pr. C. Drosten through EVA GLOBAL (https://www.european-virus-archive.com/). The Omicron BA.1 virus used in the monoclonal antibodies assay was isolated from a nasopharyngeal swab of the 1st of December in Marseille, France. The full genome sequence has been deposited on GISAID: EPI_ISL_7899754. The strain, called 2021/FR/1514, is available through EVA GLOBAL (www.european-virus-archive.com, ref: 001V-04436)

Antibodies and Sera

Post-vaccination sera: sera were collected in the context of the CORSER-4 cohort and provided by ICaReb. Sera were from individuals with previous RT-PCR confirmed COVID-19 infection and sampled one month after vaccination with one dose of Pfizer vaccine (BNT162b2, Tozinameran); individuals fully vaccinated (2 doses) with the Pfizer or AstraZeneca (ChAdOx1-S) or combination thereof and sampled at one or 6 months after the second dose; individuals fully vaccinated having received a booster dose of the Moderna vaccine (Elasomeran) and sampled at one month after the boost. Dates of vaccination and dates of sampling are provided in Table 2.

Sotrovimab/ Vir-7831 was provided by GSK (GlaxoSmithKline). Cilgavimab and Tixagevimab (AstraZeneca) were obtained from hospital pharmacy of the University hospital of La Timone (Marseille, France).

Neutralization assay with pseudotypes

The XD recombinant spike-encoding plasmid was obtained by an In-Fusion reaction (Takara) using Delta and BA.1 human codon-optimized synthetic genes as templates into the pVAX1 vector. Lentiviral particles expressing a luciferase reporter gene and pseudotyped with the ancestral (Wuhan), Delta (B.1.617.2), Omicron (BA.1) and recombinant XD spikes were produced by calcium phosphate transfection of 293T cells with plasmids provided by the Bloom laboratory [41]. The following reagent was obtained through BEI Resources, NIAID, NIH: SARS-Related Coronavirus 2, Wuhan-Hu-1 Spike-Pseudotyped Lentiviral Kit, NR-52948.

Four-fold serial dilutions of sera starting at 1:10 were mixed with 0,5 µl of pseudovirus in a final volume of 50 µl of DMEM-10% FCS during 30 min at room temperature. After incubation, 293T-ACE2 cells were added at 20,000 cells/well of a 96-well white culture plate. Luminescence was measured after 72 h using the Bright-Glo luciferase substrate and a Berthold Centro XS luminometer. Neutralization was calculated using the following formula: 1 – (RLU in presence of serum / (mean of RLU in absence of serum determined in 48 wells – 3 x STD). The effective dose 50% (ED_{50}) was determined as the serum dilution giving 50% of neutralization.

Neutralization assays with infectious virus

One day prior to infection, 5×10^4 VeroE6/TMPRSS2 cells were seeded in 100µL assay medium (containing 2.5% FCS) in 96 well culture plates. The next day, antibodies were diluted in PBS with ½ dilutions from 1000 to 0.97 ng/ml for Sotrovimab and from 5000 to 4.8 ng/ml for Cilgavimab, Tixagevimab and its combination Evusheld. Eleven 2-fold serial dilutions of antibodies in triplicate were added to the cells (25µL/well, in assay medium). Then, 25µL of a virus mix diluted in medium was added to the wells. The amount of virus working stock used was calibrated prior to the assay, based on replication kinetics, so that the viral replication was still in the exponential growth phase for the readout. Plates were first incubated 15 min at room temperature and then 2 days at 37°C prior to quantification of the viral genome by real-time RT-PCR. Synthetic RNA standards were used to quantify viral RNA abundance in copies per reaction. Viral inhibition was calculated as follows: 100* (quantity mean VC-sample quantity)/ quantity mean VC). The 50% effective concentrations (EC_{50} compound concentration required to inhibit viral RNA replication by 50%) were determined using a nonlinear regression (log(agonist) vs. response -- Variable slope (four parameters)) as described [25].

In vivo studies

Infection studies were performed in a biosafety level 3 (BSL-3) animal facility at the Institut Pasteur, in Paris. All animal work was approved by the Institut Pasteur Ethics Committee (project dap 21050) and authorized by the French Ministry of Research under project 31816 in compliance with the European and French regulations. B6.Cg-Tg(K18-Ace2)2Prlmn/J mice were purchased from The Jackson Laboratory (Maine, USA) and are bred at the Institut Pasteur under SOPF environment.

Seven- to eight-week-old mice were anesthetized by ketamine/xylazine and infected intranasally with 2 x10^4 PFU of SARS-CoV-2 isolates in 40 to 60 µl. In the first group of mice, clinical signs of disease and weight loss were monitored daily for 11 days. Four criteria (ruffled fur, hunched back posture, reduced mobility and difficulty to breath) were scored on a 0-2 scale and added up into a global clinical score. Mice were euthanized when they reached predefined endpoints (clinical score of 6 or body weight loss > 25%). A second group of infected mice was euthanized 3 days post infection (dpi) for measurement of viral load and viral titer. Right lung lobe and nasal turbinates were dissected and frozen at -80°C. Samples were homogenized in 400 µl of cold PBS using lysing matrix M (MP Biomedical) and a MP Biomedical FastPrep 24 Tissue Homogenizer. Viral RNA was extracted using an extraction robot IDEAL-32 (IDsolutions) and the NucleoMag Pathogen extraction kit (Macherey Nagel). Viral RNA quantification was performed by quantitative reverse transcription PCR (RT-qPCR) using the IP4 set of primers and probe (nCoV_IP4-14059Fw GGTAACTGGTATGATTTCG and nCoV_IP4-14146Rv CTGGTCAAGGTTAATATAGG giving a 107bp product, and nCoV_IP4-14084Probe(+) TCATACAAACCACGCCAGG [5']Hex [3']BHQ-1) and the Luna Universal Probe One-Step RT-qPCR Kit (NEB). Serial dilutions of a titrated viral stock were analysed simultaneously to express viral loads as PFU equivalents (eqPFU) per gram of tissue.

For plaque assays, 10-fold serial dilutions of samples in DMEM were added onto VeroE6 monolayers in 24 well plates. After one-hour incubation at 37°C, the inoculum was replaced with an equivalent volume of 5% FBS DMEM and 2% carboxymethylcellulose. Three days later, cells were fixed with 4% formaldehyde, followed by staining with 1% crystal violet to visualize the plaques.

Analysis of the competition assays

For each sample, we trimmed the reads using trimgalore (https://github.com/FelixKrueger/TrimGalore/tree/0.6.7). We mapped the reads on the reference sequence Wuhan-Hu-1/2019 using bwa mem (v0.7.17) [42]. We then counted the coverage of each nucleotide at all positions of the genome using bam-readcount (v1.0.0) as performed in ViralFlow [43]. We selected the SARS-CoV-2 genomic positions that differ between the sequence of the recombinant isolate (IPP08027i) and the BA.1 isolate (IPP46934i) using goalign (v0.3.5) [44], and counted the relative amounts of each nucleotide corresponding either to the recombinant XD or to the BA.1 at each of these positions.

Statistical analysis

Statistical analysis was performed using R v4.1.2 and GraphPad Prism v9. Survival curves were compared by logrank test. Viral loads and viral titers were compared by a Student's t-test. Epidemiological data of XD and Omicron cases were compared using Chi2 tests and odds ratio.

Ethical statement

As per approval by the National Ethical Committee, SPF investigation teams have continual access to personal data in order to investigate and control identified public health threats. No additional ethical clearance was needed or sought. Personal information was anonymised in this publication.

Sera from human subjects who participated in the “Sero-epidemiological study of the SARS-CoV-2 virus in France” were provided by ICAReB platform (Clinical Investigation & Access to Research Bioresources) from the center for translational science, Institut Pasteur. All participants gave written informed consent in the frame of CORSER-4 cohort after approval of the CPP Ile-de-France I Ethics Committee (2021, May 21st) and registered by the French national security agency for medicines and health products (IDRCB 2020-A00406-33) and Clinical trials (NCT 04325646).

Tables

Characteristics		N	%
Region (n=38)	Auvergne-Rhône-Alpes	4	10.50%
	Bretagne	1	2.60%
	Grand Est	4	10.50%
	Hauts-de-France	13	34.20%
	île-de-France	4	10.50%
	Normandie	3	7.90%
	Occitanie	8	21.10%
	Provence-Alpes-Côte d'Azur	1	2.60%
Sex (n=38)	Females	15	39.50%
	Males	23	60.50%
Travel history (n=34)	Yes	2	5.90%
	No	32	94.10%
Cluster (n=36)	Yes	23	63.90%
	No	13	36.10%
Previous SARS-CoV-2 infection (n=36)	Yes	2	5.60%
	No	34	94.40%
Vaccination status (n=34)	Unvaccinated	2	5.90%
	One dose	2	6%
	Two doses	21	62%
	Three doses	9	26.50%
Symptomatic infection (n=36)	Yes	36	100%
	No	0	0%
Risk factors (n=36)	Yes	12	33.30%
	No	24	66.70%
Hospitalization (n=36)	Yes	2	5.60%
	No	34	94.40%
Intensive care (n=36)	Yes	0	0%
	No	36	100%

Table 1: Characteristics of investigated cases infected by XD (N = 38). For each category, percentages were calculated over the number of cases with available data, and respective denominators are indicated in parenthesis.

	Age	Sex	Date last dose	Visit date	Vaccine
1M post 2 doses	67	F	17-06-2021	15-07-2021	PF/PF
	38	F	17-06-2021	15-07-2021	PF/PF
	50	F	22-06-2021	20-07-2021	PF/PF
	54	M	22-06-2021	20-07-2021	PF/PF
Inf/1M post 1dose	39	F	15-06-2021	27-07-2021	Inf/PF
	26	F	05-07-2021	29-07-2021	Inf/PF
	35	M	22-06-2021	13-08-2021	Inf/PF
	33	F	23-06-2021	28-07-2021	Inf/PF
6M post 2 doses	31	F	29-06-2021	15-12-2021	PF/PF
	40	M	23-06-2021	17-12-2021	PF/PF
	51	F	22-06-2021	16-12-2021	PF/PF
	51	F	13-07-2021	16-12-2021	PF/PF
	52	F	04-06-2021	25-11-2021	AZ/PF
	54	F	04-06-2021	02-12-2021	AZ/PF
	60	F	28-07-2021	15-12-2021	AZ/AZ
	61	M	18-06-2021	08-12-2021	AZ/AZ
	57	F	17-06-2021	09-12-2021	AZ/AZ
	61	M	23-06-2021	15-12-2021	AZ/AZ
1M post 3 doses	51	F	16-12-2021	11-01-2022	PF/PF/MO
	40	M	17-12-2021	11-01-2022	PF/PF/MO
	31	F	15-12-2021	11-01-2022	PF/PF/MO
	51	F	16-12-2021	11-01-2022	PF/PF/MO
	52	F	01-12-2021	06-01-2022	AZ/PF/PF
	54	F	02-12-2021	04-01-2022	AZ/PF/PF
	61	M	08-12-2021	05-01-2022	AZ/AZ/PF
	57	F	09-12-2021	06-01-2022	AZ/AZ/PF
	60	F	27-12-2021	11-01-2022	AZ/AZ/MO
	61	M	15-12-2021	11-01-2022	AZ/AZ/MO

Table 2: Characteristics of the serum donors.

			virus			
Antibody			B.1	AY.4	BA.1	XD
GSK/ Vir	Sotrovimab (vir-7831)	EC_{50}	62,7	218,1	163,7	317,5
		fold-change	-	3,5	2,6	5,1
AstraZeneca	Cilgavimab (AZD1061)	EC_{50}	29,7	47,7	501,1	402,8
		fold-change	-	1,6	16,9	13,5
	Tixagevimab (AZD8895)	EC_{50}	62,7	218,1	n.n	n.n
		fold-change	-	3,5	-	-
	Evusheld (AZD7442)	EC_{50}	16,8	11,9	617,4	637,8
		fold-change	-	0,7	36,7	37,9

Table 3: Interpolated EC_{50} values of therapeutic antibodies against SARS-CoV-2 BavPat1, Delta (AY.4), Omicron (BA.1) and the recombinant (XD) virus. EC_{50} values are expressed in ng/mL.

Declarations

Data availability

All data supporting the findings of this study are available in the manuscript. The SARS-CoV-2 genomic data analysed here are available on GISAID (https://www.gisaid.org/).

Acknowledgments

We would like to thank all the healthcare workers, public health employees, and scientists involved in the COVID-19 response. We acknowledge the authors, originating and submitting laboratories of the sequences from GISAID and GenBank (Supplementary Table 1). We thank the Institut Pasteur C2RA Animal Facility staff for their dedication to breeding and care of mice, the team of the Mutualized Platform for Microbiology at Institut Pasteur, Dr Justine Schaeffer for scientific discussions, and Dr Cécile Baronti and Dr Boris Pastorino for virus production and neutralizing activity experiments. We acknowledge our colleagues of the Danish Covid-19 Genomics Consortium (www.covid19genomics.dk/about), and our colleagues from the Covid19seq group of the Wisplinghoff Laboratories. We are grateful to Anaïs Perilhou, Sandrine Fernandes Pellerin, Yanis Dahoumane and Tan-Phuc Buivan from the center for translational science, Institut Pasteur, for the preparation and the

management of the cohort, to Laurence Arowas, Ayla Zayoud, Emmanuel Roux, Alain Li, Sophie Vacant, Sophie Chaouche and Remy Yim of ICAReB platform from the Center for Translational Science, at the Institut Pasteur for the management of the biobank for providing sera samples from donors. We acknowledge the European virus archive-Marseille (EVAM, technological platforms of Aix-Marseille university) for providing a BA.1 Omicron isolate. This work used the computational and storage services provided by the IT department at Institut Pasteur, Paris.

Funding

This study has received funding from the EMERGEN programme (projects BIOVAR and MODVAR), from Institut Pasteur, Santé publique France (the French national public health agency), the French Government's Investissement d'Avenir programme, Laboratoire d'Excellence “Integrative Biology of Emerging Infectious Diseases” (grant n°ANR-10-LABX-62-IBEID), REACTing (Research & Action Emerging Infectious Diseases), the “Enhancing Whole Genome Sequencing (WGS) and/or Reverse Transcription Polymerase Chain Reaction (RT-PCR) national infrastructures and capacities to respond to the COVID-19 pandemic in the European Union and European Economic Area” Grant Agreement ECDC/HERA/2021/007 ECD. 12221, the RECOVER project funded by the European Union’s Horizon 2020 research and innovation programme under grant agreement No. 101003589 and the Caisse nationale d’assurance maladie (Cnam), the national health insurance funds. ESL acknowledges funding from the INCEPTION programme (Investissements d’Avenir grant ANR-16-CONV-0005).

Competing interests

AZ, TD and SK are employed by Inovie GEN-BIO. CS is employed by Dr. Wisplinghoff laboratories. NC and HL are employed by BioPath. MPB, and AEB are employed by inBiome B.V.

Author contribution

Experimental strategy design, experiments: X.M., XdL, S.W. and E.S.-L. Data acquisition and curation: F.D., A.B., O.D., V.G., S.N., M.Be., J.Fo., M.R., S.K., A.Z., T.D., S.B., V.E., C.R., S.F., J-M.P., N.C., H.L., E.A-G., F.J., L.G., V.B., H.M., M.P.B., M.W., C.S., S.P., L.J., S.E-K., J.Fu., Y.Y. Vital materials: C.C., B.Cou., S.M-J., A.P., M.-C.H.-B. Initial identification of the recombinant: S.N. Phylogenetic analysis: F.L., J.B., and E.S.-L. Virus isolation, production, titration: F.D., A.B., O.D. Structural modelling: F.A.R. Infectious virus neutralization assays: F.T, X.dL. Pseudovirus neutralization assays: S.M., M.A., F.A. S.vdW. Infection experiments in mice and analysis: M.P., L.C., L.L., D., F.L., E.S.-L. and X.M. The Emergen consortium provided the framework for the SARS-CoV-2 genomic surveillance in France. Writing - Original draft: E.S.-L. Writing – review and editing: X.M., S.vdW., F.L., J.B.,V.G., F.T., X.dL., B.Coi., F.A.R., A.M. with inputs from all authors.

References

1 Worobey, M. & Holmes, E. C. Evolutionary aspects of recombination in RNA viruses. *J Gen Virol* **80 (Pt 10)**, 2535-2543, doi:10.1099/0022-1317-80-10-2535 (1999).

2 Simon-Loriere, E. & Holmes, E. C. Why do RNA viruses recombine? *Nat Rev Microbiol* **9**, 617-626, doi:10.1038/nrmicro2614 (2011).

3 WHO. *Tracking SARS-CoV-2 variants*, <https://www.who.int/en/activities/tracking-SARS-CoV-2-variants/> (2022).

4 Viana, R. *et al.* Rapid epidemic expansion of the SARS-CoV-2 Omicron variant in southern Africa. *Nature*, doi:10.1038/s41586-022-04411-y (2022).

5 Plante, J. A. *et al.* Spike mutation D614G alters SARS-CoV-2 fitness. *Nature* **592**, 116-121, doi:10.1038/s41586-020-2895-3 (2021).

6 Saito, A. *et al.* Enhanced fusogenicity and pathogenicity of SARS-CoV-2 Delta P681R mutation. *Nature* **602**, 300-306, doi:10.1038/s41586-021-04266-9 (2022).

7 Syed, A. M. *et al.* Rapid assessment of SARS-CoV-2-evolved variants using virus-like particles. *Science* **374**, 1626-1632, doi:10.1126/science.abl6184 (2021).

8 Boni, M. F. *et al.* Evolutionary origins of the SARS-CoV-2 sarbecovirus lineage responsible for the COVID-19 pandemic. *Nat Microbiol* **5**, 1408-1417, doi:10.1038/s41564-020-0771-4 (2020).

9 Lytras, S. *et al.* Exploring the Natural Origins of SARS-CoV-2 in the Light of Recombination. *Genome Biol Evol* **14**, doi:10.1093/gbe/evac018 (2022).

10 Gutierrez, B. *et al.* Emergence and widespread circulation of a recombinant SARS-CoV-2 lineage in North America. *medRxiv*, 2021.2011.2019.21266601, doi:10.1101/2021.11.19.21266601 (2021).

11 Jackson, B. *et al.* Generation and transmission of interlineage recombinants in the SARS-CoV-2 pandemic. *Cell* **184**, 5179-5188 e5178, doi:10.1016/j.cell.2021.08.014 (2021).

12 VanInsberghe, D., Neish, A. S., Lowen, A. C. & Koelle, K. Recombinant SARS-CoV-2 genomes circulated at low levels over the first year of the pandemic. *Virus Evolution* **7**, veab059, doi:10.1093/ve/veab059 (2021).

13 Wertheim, J. O. *et al.* Capturing intrahost recombination of SARS-CoV-2 during superinfection with Alpha and Epsilon variants in New York City. *medRxiv*, 2022.2001.2018.22269300, doi:10.1101/2022.01.18.22269300 (2022).

14 O'Toole, A. *et al.* Assignment of epidemiological lineages in an emerging pandemic using the pangolin tool. *Virus Evol* **7**, veab064, doi:10.1093/ve/veab064 (2021).

15 Aksamentov, I., Roemer, C., Hodcroft, E. B. & Neher, R. A. Nextclade: clade assignment, mutation calling and quality control for viral genomes. *Journal of Open Source Software* **6**, 3773, doi:10.21105/joss.03773 (2021).

16 Nguyen, S. V. (2022).

17 ECDC. *SARS-CoV-2 variants of concern as of 24 March 2022*, <https://www.ecdc.europa.eu/en/covid-19/variants-concern> (2022).

18 Maisa, A. *et al.* First cases of Omicron in France are exhibiting mild symptoms, November 2021-January 2022. *Infect Dis Now*, doi:10.1016/j.idnow.2022.02.003 (2022).

19 Elbe, S. & Buckland-Merrett, G. Data, disease and diplomacy: GISAID's innovative contribution to global health. *Glob Chall* **1**, 33-46, doi:10.1002/gch2.1018 (2017).

20 Simon-Loriere, E., Rossolillo, P. & Negroni, M. RNA structures, genomic organization and selection of recombinant HIV. *RNA Biol* **8**, 280-286, doi:10.4161/rna.8.2.15193 (2011).

21 Muslin, C., Mac Kain, A., Bessaud, M., Blondel, B. & Delpeyroux, F. Recombination in Enteroviruses, a Multi-Step Modular Evolutionary Process. *Viruses* **11**, doi:10.3390/v11090859 (2019).

22 Simon-Loriere, E. & Schwartz, O. Towards SARS-CoV-2 serotypes? *Nat Rev Microbiol* **20**, 187-188, doi:10.1038/s41579-022-00708-x (2022).

23 Cao, Y. *et al.* Omicron escapes the majority of existing SARS-CoV-2 neutralizing antibodies. *Nature*, doi:10.1038/s41586-021-04385-3 (2021).

24 Planas, D. *et al.* Considerable escape of SARS-CoV-2 Omicron to antibody neutralization. *Nature*, doi:https://doi.org/10.1038/d41586-021-03827-2 (2021).

25 Touret, F., Baronti, C., Bouzidi, H. S. & de Lamballerie, X. In vitro evaluation of therapeutic antibodies against a SARS-CoV-2 Omicron B.1.1.529 isolate. *Sci Rep* **12**, 4683, doi:10.1038/s41598-022-08559-5 (2022).

26 Ulloa, A. C., Buchan, S. A., Daneman, N. & Brown, K. A. Estimates of SARS-CoV-2 Omicron Variant Severity in Ontario, Canada. *JAMA*, doi:10.1001/jama.2022.2274 (2022).

27 Wolter, N. *et al.* Early assessment of the clinical severity of the SARS-CoV-2 omicron variant in South Africa: a data linkage study. *Lancet* **399**, 437-446, doi:10.1016/S0140-6736(22)00017-4 (2022).

28 Shuai, H. *et al.* Attenuated replication and pathogenicity of SARS-CoV-2 B.1.1.529 Omicron. *Nature*, doi:10.1038/s41586-022-04442-5 (2022).

29 Halfmann, P. J. *et al.* SARS-CoV-2 Omicron virus causes attenuated disease in mice and hamsters. *Nature*, doi:10.1038/s41586-022-04441-6 (2022).

30 Tyson, J. R. *et al.* Improvements to the ARTIC multiplex PCR method for SARS-CoV-2 genome sequencing using nanopore. *bioRxiv*, 2020.2009.2004.283077, doi:10.1101/2020.09.04.283077 (2020).

31 Matranga, C. B. *et al.* Enhanced methods for unbiased deep sequencing of Lassa and Ebola RNA viruses from clinical and biological samples. *Genome Biol* **15**, 519, doi:10.1186/PREACCEPT-1698056557139770 (2014).

32 Grubaugh, N. D. *et al.* An amplicon-based sequencing framework for accurately measuring intrahost virus diversity using PrimalSeq and iVar. *Genome Biol* **20**, 8, doi:10.1186/s13059-018-1618-7 (2019).

33 Li, H. *et al.* The Sequence Alignment/Map format and SAMtools. *Bioinformatics* **25**, 2078-2079, doi:10.1093/bioinformatics/btp352 (2009).

34 Hadfield, J. *et al.* Nextstrain: real-time tracking of pathogen evolution. *Bioinformatics* **34**, 4121-4123, doi:10.1093/bioinformatics/bty407 (2018).

35 Hoang, D. T., Chernomor, O., von Haeseler, A., Minh, B. Q. & Vinh, L. S. UFBoot2: Improving the Ultrafast Bootstrap Approximation. *Mol Biol Evol* **35**, 518-522, doi:10.1093/molbev/msx281 (2018).

36 Minh, B. Q. *et al.* IQ-TREE 2: New Models and Efficient Methods for Phylogenetic Inference in the Genomic Era. *Mol Biol Evol* **37**, 1530-1534, doi:10.1093/molbev/msaa015 (2020).

37 Kalyaanamoorthy, S., Minh, B. Q., Wong, T. K. F., von Haeseler, A. & Jermiin, L. S. ModelFinder: fast model selection for accurate phylogenetic estimates. *Nat Methods* **14**, 587-589, doi:10.1038/nmeth.4285 (2017).

38 Martin, D. P. *et al.* RDP5: A computer program for analysing recombination in, and removing signals of recombination from, nucleotide sequence datasets. *Virus Evol*, veaa087, doi:10.1093/ve/veaa087 (2020).

39 Lam, H. M., Ratmann, O. & Boni, M. F. Improved Algorithmic Complexity for the 3SEQ Recombination Detection Algorithm. *Mol Biol Evol* **35**, 247-251, doi:10.1093/molbev/msx263 (2018).

40 Lescure, F. X. *et al.* Clinical and virological data of the first cases of COVID-19 in Europe: a case series. *Lancet Infect Dis* **20**, 697-706, doi:10.1016/S1473-3099(20)30200-0 (2020).

41 Crawford, K. H. D. *et al.* Protocol and Reagents for Pseudotyping Lentiviral Particles with SARS-CoV-2 Spike Protein for Neutralization Assays. *Viruses* **12**, doi:10.3390/v12050513 (2020).

42 Li, H. & Durbin, R. Fast and accurate short read alignment with Burrows-Wheeler transform. *Bioinformatics* **25**, 1754-1760, doi:10.1093/bioinformatics/btp324 (2009).

43 Dezordi, F. Z. *et al.* ViralFlow: A Versatile Automated Workflow for SARS-CoV-2 Genome Assembly, Lineage Assignment, Mutations and Intrahost Variant Detection. *Viruses* **14**, doi:10.3390/v14020217 (2022).

44 Lemoine, F. & Gascuel, O. Gotree/Goalign: toolkit and Go API to facilitate the development of phylogenetic workflows. *NAR Genom Bioinform* **3**, lqab075, doi:10.1093/nargab/lqab075 (2021).

Figures

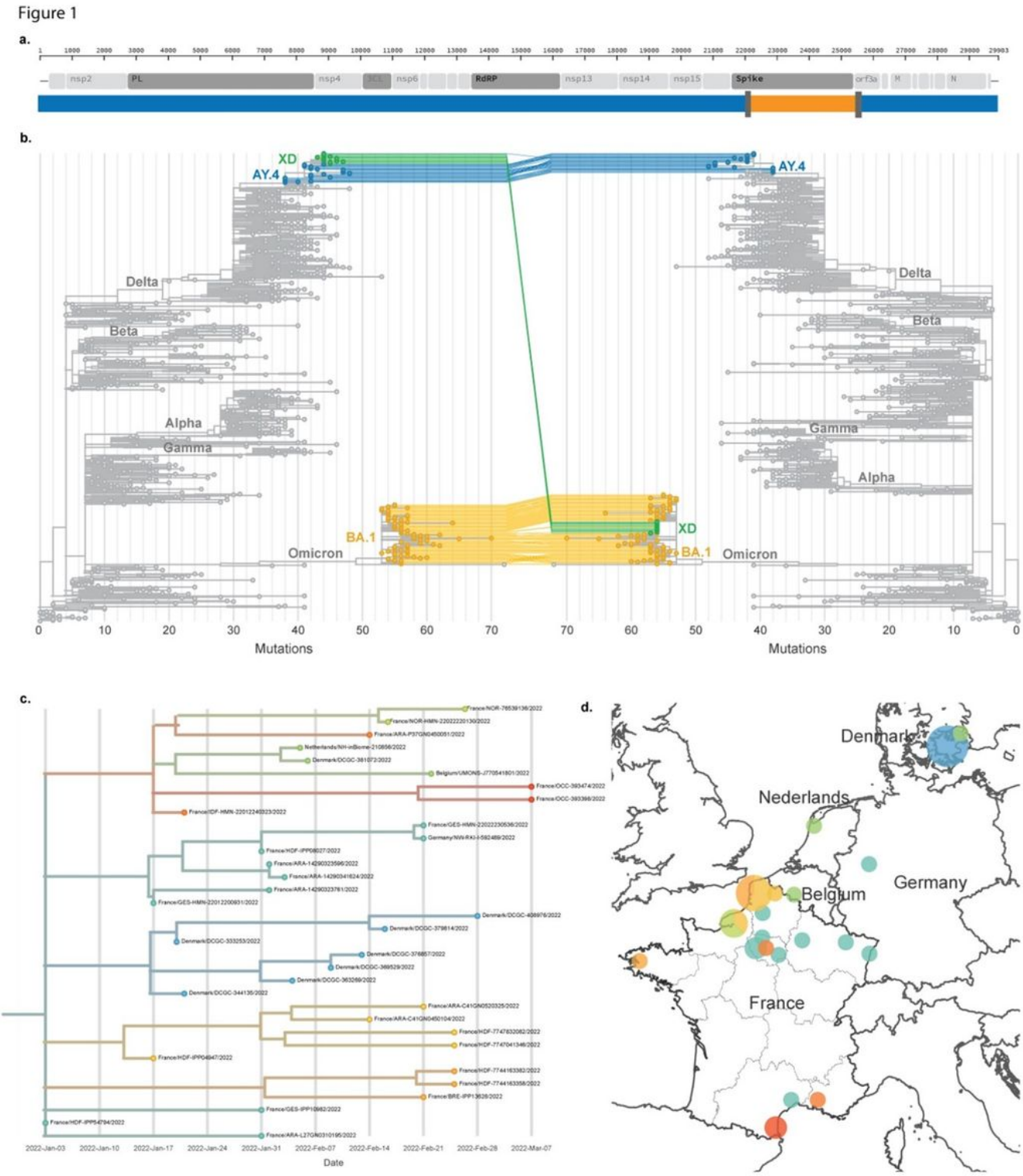

Figure 1

Mosaic genome and initial detection of the XD lineage. a. Scheme of the XD virus genome. The Delta-like regions are shown in blue, and the BA.1 region in orange. The windows corresponding to the recombination breakpoint are shown in dark grey. b. Maximum likelihood phylogenies of regions of the recombinant genome corresponding to either Delta (left) or Omicron BA.1 (right). c. Time resolved phylogeny of the XD lineage and d. geographic distribution.

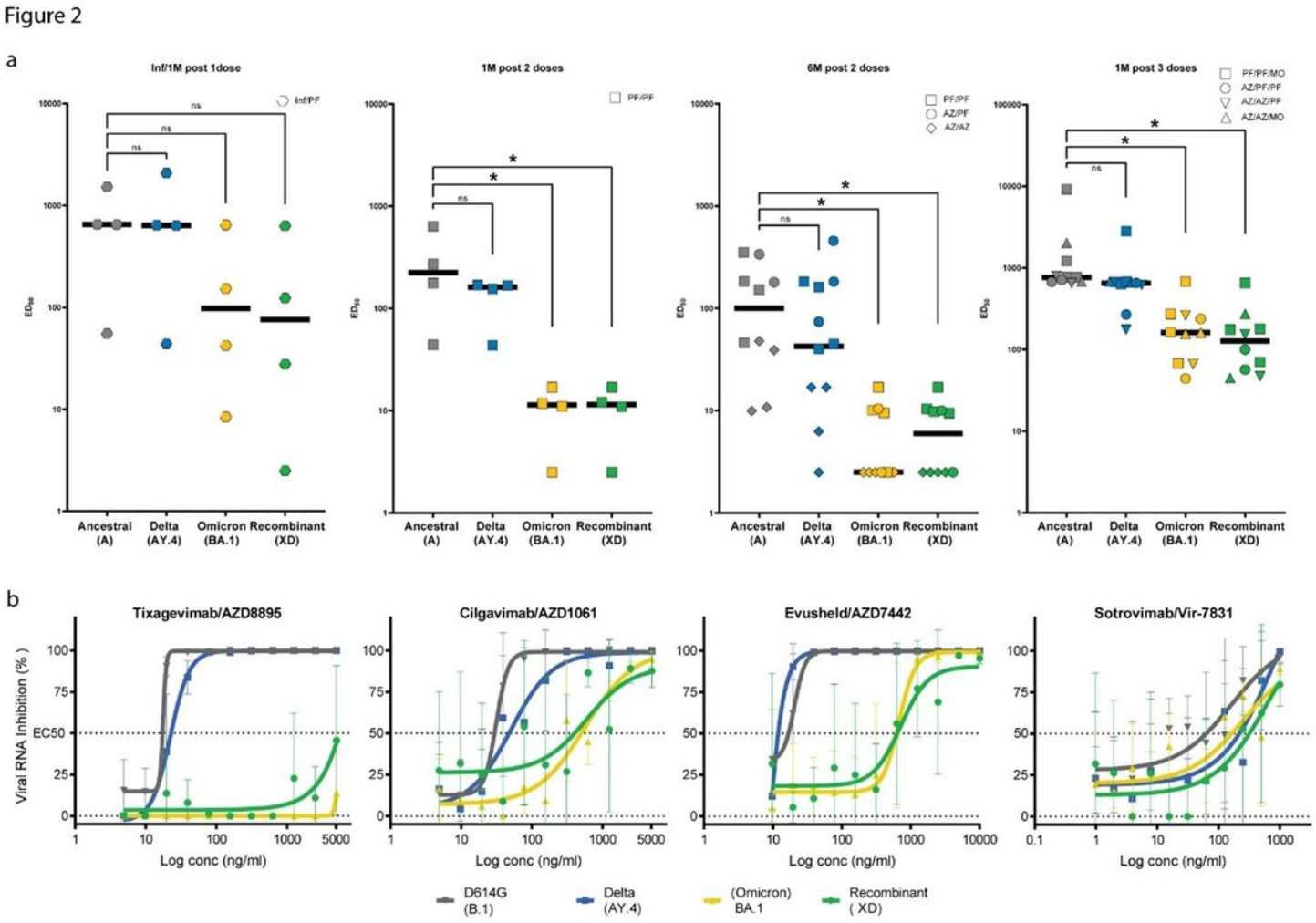

Figure 2

XD recombinant and immune escape. a. Pseudovirus neutralization titers of sera from vaccine recipients or individuals infected and vaccinated. **b.** Dose response curves showing the susceptibility of the XD virus to a panel of therapeutic monoclonal antibodies. Data presented here correspond to 3 technical replicates in VeroE6-TMPRSS2 cells, and error bars show mean ± s.d. A schematic of the XD spike mutations in comparison to the parental sequences is shown in Extended Data Fig. 4.

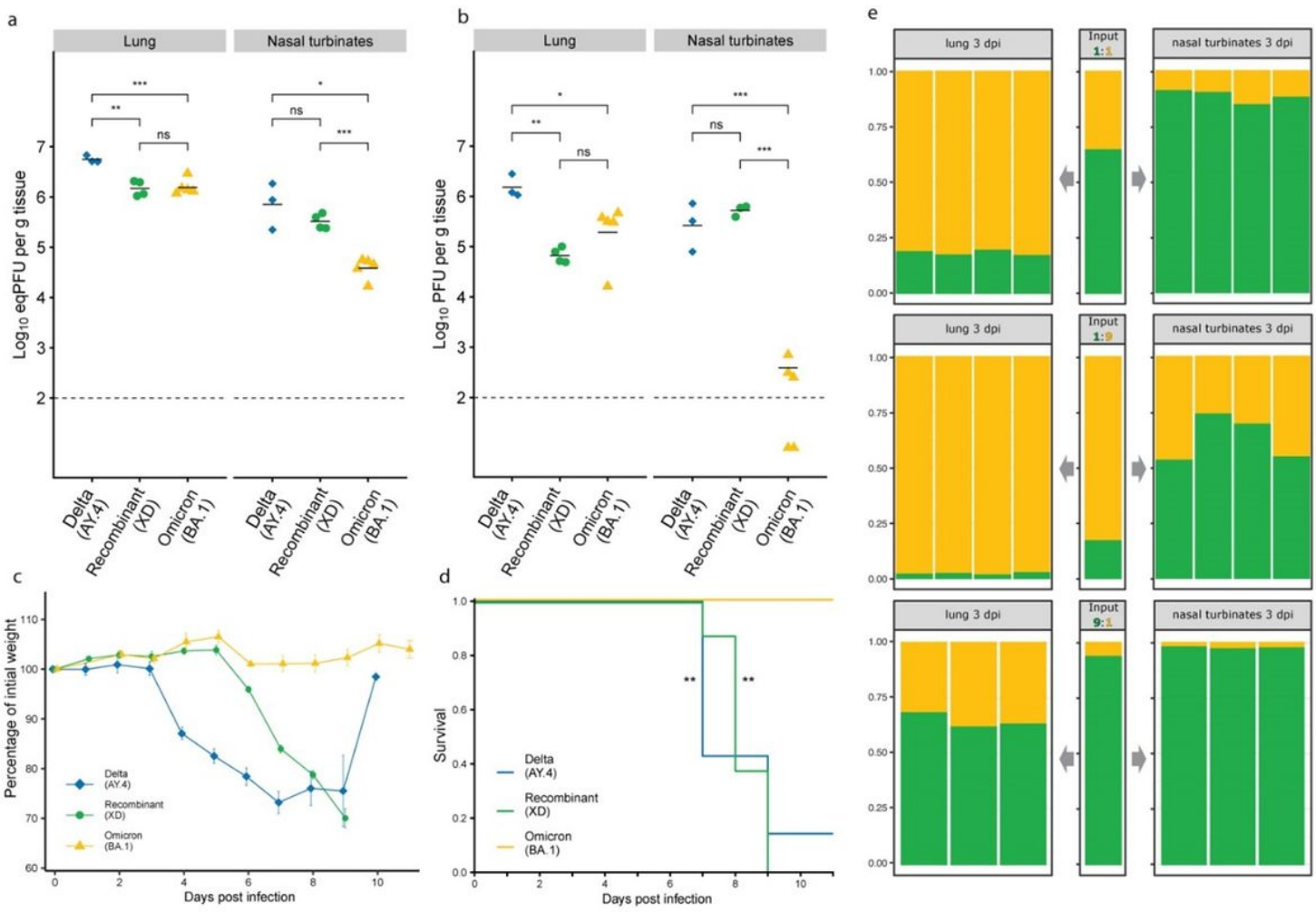

Figure 3

Phenotypic differences of XD and parental viruses in K18-hACE2 mice. a. Viral RNA level and **b.** infectious virus titer, in the lungs and nasal turbinates of K18-hACE2 mice inoculated with Delta AY.4 (n= 3, blue), XD recombinant (n= 4, green) and Omicron BA.1 (n= 4, yellow) at 3 dpi. **c.** Weight change (mean ± sem) and **d.** survival of K18-hACE2 mice inoculated with Delta AY.4 (n= 7, blue), XD recombinant (n= 8, green) and Omicron BA.1 (n= 6, yellow). **e.** Proportion of XD (green) and BA.1 (yellow) inoculated (center) and measured in the lungs (left) and nasal turbinates (right) of K18-ACE2 mice (each bar of the panels is an independent mouse).

Supplementary Files

This is a list of supplementary files associated with this preprint. Click to download.

- SupplTable1GISAIDacknowledgements.pdf
- extendeddata.docx